

Supporting materials

Protonated and deprotonated vanadyl imidazole tartrates for the mimics of the vanadium coordination in FeV-cofactor of V-nitrogenase

Shuang-Shuang Zhu,^{‡a} Zhen-Lang Xie,^{‡a} Lan Deng,^a Si-Yuan Wang,^a Lu-Bin Ni,^b Zhao-Hui Zhou^{*a}

^aState Key Laboratory of Physical Chemistry of Solid Surfaces and Department of Chemistry, College of Chemistry and Chemical Engineering, Xiamen University, Xiamen, 361005, China. Tel: + 86-592-2184531; Fax: + 86-592-2183047; Email: zhzhou@xmu.edu.cn

^bSchool of Chemistry and Chemical Engineering, Yangzhou University, Yangzhou 225002 Jiangsu, China.

[‡]These authors contributed equally to this work.

Figure and Table Options

Figure S1. 2D layered structure of $(\text{H}_2\text{im})_2[\Delta, \Lambda\text{-V}^{\text{IV}}_2\text{O}_2(\text{R,R-H}_2\text{tart})(\text{R,R-tart})(\text{Him})_2] \cdot \text{Him}$ (1).	4
Figure S2. 2D layered structure of $[\Lambda, \Lambda\text{-V}^{\text{IV}}_2\text{O}_2(\text{R,R-tart})(\text{Him})_6] \cdot 4\text{H}_2\text{O}$ (2).	5
Figure S3. ORTEP plot of the anion structure $(\text{H}_2\text{im})_2[\Lambda, \Delta\text{-V}^{\text{IV}}_2\text{O}_2(\text{S,S-H}_2\text{tart})(\text{S,S-tart})(\text{Him})_2] \cdot \text{Him}$ (3) at the 30% probability levels.	6
Figure S4. ORTEP plot of the molecular structure $[\Delta, \Delta\text{-V}^{\text{IV}}_2\text{O}_2(\text{S,S-tart})(\text{Him})_6] \cdot 4\text{H}_2\text{O}$ (4) at the 30% probability levels.	7
Figure S5. Chemdraw structures for oxidovanadium tartrates 5 – 8 , other oxidovanadium hydroxycarboxylates 9 – 16 and reported FeV-cos 17 – 21	8
Figure S6. FT-IR spectrum of <i>R,R</i> -tartaric acid originated from Spectral Database for Organic Compounds SDBS. URL for this compound: https://sdb.sdb.aist.go.jp/sdb/cgi-bin/landingpage?sdbno=1071	9
Figure S7. FT-IR spectrum of <i>S,S</i> -tartaric acid originated from Spectral Database for Organic Compounds SDBS. URL for this compound: https://sdb.sdb.aist.go.jp/sdb/cgi-bin/landingpage?sdbno=488	10
Figure S8a. VCD and IR spectra of $(\text{H}_2\text{im})_2[\Delta, \Lambda\text{-V}^{\text{IV}}_2\text{O}_2(\text{R,R-H}_2\text{tart})(\text{R,R-tart})(\text{Him})_2] \cdot \text{Him}$ (1) with KBr pellet.	11

Figure S8b. VCD and IR spectra of $[\Lambda,\Lambda\text{-V}^{\text{IV}}_2\text{O}_2(R,R\text{-tart})(\text{Him})_6]\cdot 4\text{H}_2\text{O}$ (2) with KBr pellet.	12
Figure S8c. VCD and IR spectra of $(\text{H}_2\text{im})_2[\Lambda,\Lambda\text{-V}^{\text{IV}}_2\text{O}_2(S,S\text{-H}_2\text{tart})(S,S\text{-tart})(\text{Him})_2]\cdot \text{Him}$ (3) with KBr pellet.	13
Figure S8d. VCD and IR spectra of $[\Delta,\Delta\text{-V}^{\text{IV}}_2\text{O}_2(S,S\text{-tart})(\text{Him})_6]\cdot 4\text{H}_2\text{O}$ (4) with KBr pellet.	14
Figure S9. X-band EPR spectra of 1 and 3 in solid-states (a) and 1 in H_2O (b) at 298 K, respectively.....	15
Figure S10. X-band EPR spectra with <i>g</i> -axis in solid state of 1 – 4 at 298 K, respectively... 16	
Figure S11. Temperature-dependence magnetic susceptibility of 2 in an applied field of $B = 0.1$ T over the range of 2 – 300 K. Red line correspond to the best fitting result.....	17
Figure S12. IR spectra of $(\text{H}_2\text{im})_2[\Delta,\Lambda\text{-V}^{\text{IV}}_2\text{O}_2(R,R\text{-H}_2\text{tart})(R,R\text{-tart})(\text{Him})_2]\cdot \text{Him}$ (1), $[\Lambda,\Lambda\text{-V}^{\text{IV}}_2\text{O}_2(R,R\text{-tart})(\text{Him})_6]\cdot 4\text{H}_2\text{O}$ (2), $(\text{H}_2\text{im})_2[\Lambda,\Delta\text{-V}^{\text{IV}}_2\text{O}_2(S,S\text{-H}_2\text{tart})(S,S\text{-tart})(\text{Him})_2]\cdot \text{Him}$ (3) and $[\Delta,\Delta\text{-V}^{\text{IV}}_2\text{O}_2(S,S\text{-tart})(\text{Him})_6]\cdot 4\text{H}_2\text{O}$ (4), respectively.....	18
Figure S13. (a) Diffused reflectance UV-Vis spectra of solids $(\text{H}_2\text{im})_2[\Delta,\Lambda\text{-V}^{\text{IV}}_2\text{O}_2(R,R\text{-H}_2\text{tart})(R,R\text{-tart})(\text{Him})_2]\cdot \text{Him}$ (1), $[\Lambda,\Lambda\text{-V}^{\text{IV}}_2\text{O}_2(R,R\text{-tart})(\text{Him})_6]\cdot 4\text{H}_2\text{O}$ (2), $(\text{H}_2\text{im})_2[\Lambda,\Delta\text{-V}^{\text{IV}}_2\text{O}_2(S,S\text{-H}_2\text{tart})(S,S\text{-tart})(\text{Him})_2]\cdot \text{Him}$ (3) and $[\Delta,\Delta\text{-V}^{\text{IV}}_2\text{O}_2(S,S\text{-tart})(\text{Him})_6]\cdot 4\text{H}_2\text{O}$ (4), respectively. (b) Comparisons for solid and solution UV-Vis spectrum of $[\Lambda,\Lambda\text{-V}^{\text{IV}}_2\text{O}_2(R,R\text{-tart})(\text{Him})_6]\cdot 4\text{H}_2\text{O}$ (2) in water (inset: UV-Vis spectra with local amplification regions).	19
Figure S14. TG–DTG curves of $(\text{H}_2\text{im})_2[\Delta,\Lambda\text{-V}^{\text{IV}}_2\text{O}_2(R,R\text{-H}_2\text{tart})(R,R\text{-tart})(\text{Him})_2]\cdot \text{Him}$ (1 , a); TG–DTG curves of $[\Lambda,\Lambda\text{-V}^{\text{IV}}_2\text{O}_2(R,R\text{-tart})(\text{Him})_6]\cdot 4\text{H}_2\text{O}$ (2 , b); TG–DTG curves of $(\text{H}_2\text{im})_2[\Lambda,\Delta\text{-V}^{\text{IV}}_2\text{O}_2(S,S\text{-H}_2\text{tart})(S,S\text{-tart})(\text{Him})_2]\cdot \text{Him}$ (3 , c); TG–DTG curves of $[\Delta,\Delta\text{-V}^{\text{IV}}_2\text{O}_2(S,S\text{-tart})(\text{Him})_6]\cdot 4\text{H}_2\text{O}$ (4 , d).	20
Figure S15. Cyclic voltammogram of $[\Lambda,\Lambda\text{-V}_2\text{O}_2(R,R\text{-tart})(\text{Him})_6]\cdot 4\text{H}_2\text{O}$ (2) in anhydrous DMF with 0.10 M $[\text{n-Bu}_4\text{N}]\text{ClO}_4$ at a glassy carbon electrode with scan rate of $50 \text{ mV}\cdot\text{s}^{-1}$ (a) and various scan rates (b), respectively. (c) Plots of redox peak currents against $v^{1/2}$. (d) Differential pulse voltammogram of 2	21
Figure S16. Comparison of the observed PXRD (red) with the simulated patterns (black) calculated from the crystal data for $[\Lambda,\Lambda\text{-V}^{\text{IV}}_2\text{O}_2(R,R\text{-tart})(\text{Him})_6]\cdot 4\text{H}_2\text{O}$ (2).	22
Table S1. Crystallographic data and structural refinements for complexes $(\text{H}_2\text{im})_2[\Delta,\Lambda\text{-V}^{\text{IV}}_2\text{O}_2(R,R\text{-H}_2\text{tart})(R,R\text{-tart})(\text{Him})_2]\cdot \text{Him}$ (1), $[\Lambda,\Lambda\text{-V}^{\text{IV}}_2\text{O}_2(R,R\text{-tart})(\text{Him})_6]\cdot 4\text{H}_2\text{O}$ (2), $(\text{H}_2\text{im})_2[\Lambda,\Delta\text{-V}^{\text{IV}}_2\text{O}_2(S,S\text{-H}_2\text{tart})(S,S\text{-tart})(\text{Him})_2]\cdot \text{Him}$ (3) and $[\Delta,\Delta\text{-V}^{\text{IV}}_2\text{O}_2(S,S\text{-tart})(\text{Him})_6]\cdot 4\text{H}_2\text{O}$ (4), respectively.....	23
Table S2. Selected hydrogen bonds (Å) in $(\text{H}_2\text{im})_2[\Delta,\Lambda\text{-V}^{\text{IV}}_2\text{O}_2(R,R\text{-H}_2\text{tart})(R,R\text{-tart})(\text{Him})_2]\cdot \text{Him}$ (1).	25
Table S3. Selected hydrogen bonds (Å) in $[\Lambda,\Lambda\text{-V}^{\text{IV}}_2\text{O}_2(R,R\text{-tart})(\text{Him})_6]\cdot 4\text{H}_2\text{O}$ (2).	26

Table S4. Selected hydrogen bonds (Å) in $(\text{H}_2\text{im})_2[\Lambda,\Delta\text{-V}^{\text{IV}}_2\text{O}_2(\text{S,S-H}_2\text{tart})(\text{S,S-tart})(\text{Him})_2]\cdot\text{Him}$ (3).....	27
Table S5. Selected hydrogen bonds (Å) in $[\Delta,\Delta\text{-V}^{\text{IV}}_2\text{O}_2(\text{S,S-tart})(\text{Him})_6]\cdot 4\text{H}_2\text{O}$ (4).....	28
Table S6. Selected bond distances (Å) and angles (°) for $(\text{H}_2\text{im})_2[\Delta,\Lambda\text{-V}^{\text{IV}}_2\text{O}_2(\text{R,R-H}_2\text{tart})(\text{R,R-tart})(\text{Him})_2]\cdot\text{Him}$ (1).....	29
Table S7. Selected bond distances (Å) and angles (°) for $[\Lambda,\Lambda\text{-V}^{\text{IV}}_2\text{O}_2(\text{R,R-tart})(\text{Him})_6]\cdot 4\text{H}_2\text{O}$ (2).....	30
Table S8. Selected bond distances (Å) and angles (°) for $(\text{H}_2\text{im})_2[\Lambda,\Delta\text{-V}^{\text{IV}}_2\text{O}_2(\text{S,S-H}_2\text{tart})(\text{S,S-tart})(\text{Him})_2]\cdot\text{Him}$ (3).....	31
Table S9. Selected bond distances (Å) and angles (°) for $[\Delta,\Delta\text{-V}^{\text{IV}}_2\text{O}_2(\text{S,S-tart})(\text{Him})_6]\cdot 4\text{H}_2\text{O}$ (4).....	32
Table S10a. The formulas of oxidovanadium tartrates 1 – 18 , other oxidovanadium hydroxycarboxylates 19 – 38 and reported FeV-cos 39 – 43	33
Table S10b. Comparisons of selected bond distances (Å) for oxidovanadium tartrates 1 – 18 , other oxidovanadium hydroxycarboxylates 19 – 38 and reported FeV-cos 39 – 43	34
Table S11. Comparisons of Mo–O distances (Å) in typical molybdenum citrates with bridging sulfur/oxygen atom.....	36
Table S12. Bond valence calculations for complexes $(\text{H}_2\text{im})_2[\Delta,\Lambda\text{-V}^{\text{IV}}_2\text{O}_2(\text{R,R-H}_2\text{tart})(\text{R,R-tart})(\text{Him})_2]\cdot\text{Him}$ (1), $[\Lambda,\Lambda\text{-V}^{\text{IV}}_2\text{O}_2(\text{R,R-tart})(\text{Him})_6]\cdot 4\text{H}_2\text{O}$ (2), $(\text{H}_2\text{im})_2[\Lambda,\Delta\text{-V}^{\text{IV}}_2\text{O}_2(\text{S,S-H}_2\text{tart})(\text{S,S-tart})(\text{Him})_2]\cdot\text{Him}$ (3) and $[\Delta,\Delta\text{-V}^{\text{IV}}_2\text{O}_2(\text{S,S-tart})(\text{Him})_6]\cdot 4\text{H}_2\text{O}$ (4), respectively. .	37

Figure S1. 2D layered structure of $(\text{H}_2\text{im})_2[\Delta,\Lambda\text{-V}^{\text{IV}}\text{O}_2(\text{R,R-H}_2\text{tart})(\text{R,R-tart})(\text{Him})_2] \cdot \text{Him}$ (**1**).

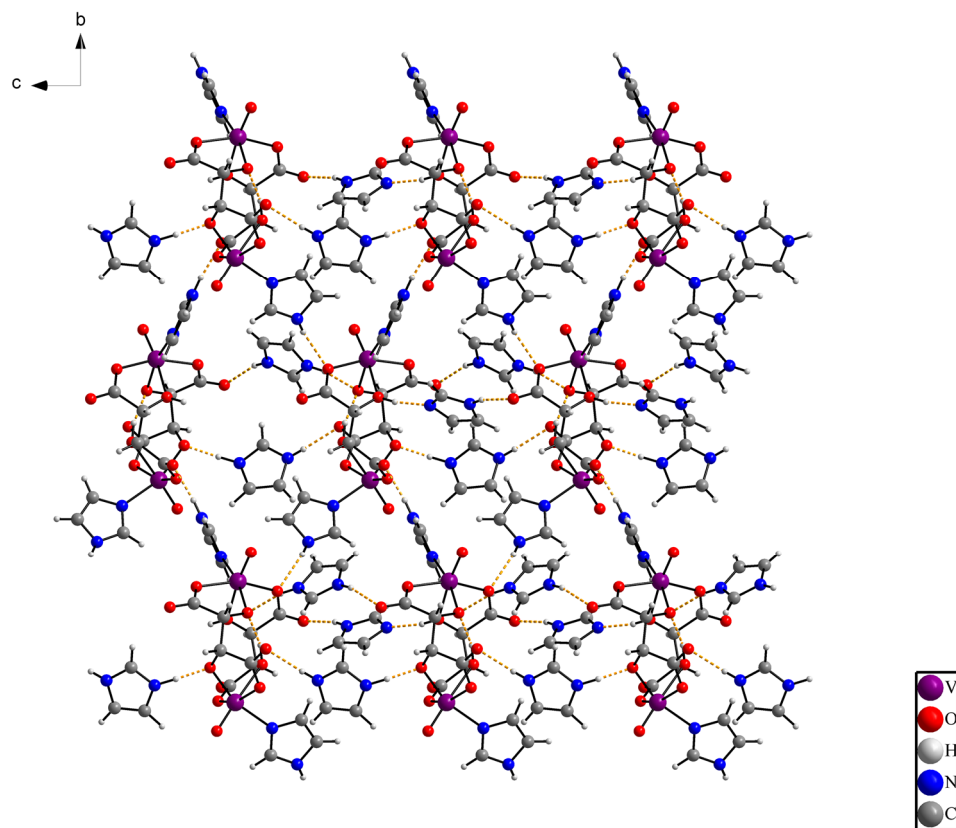


Figure S2. 2D layered structure of $[\Lambda,\Lambda\text{-V}^{\text{IV}}_2\text{O}_2(\text{R,R-tart})(\text{Him})_6]\cdot 4\text{H}_2\text{O}$ (**2**).

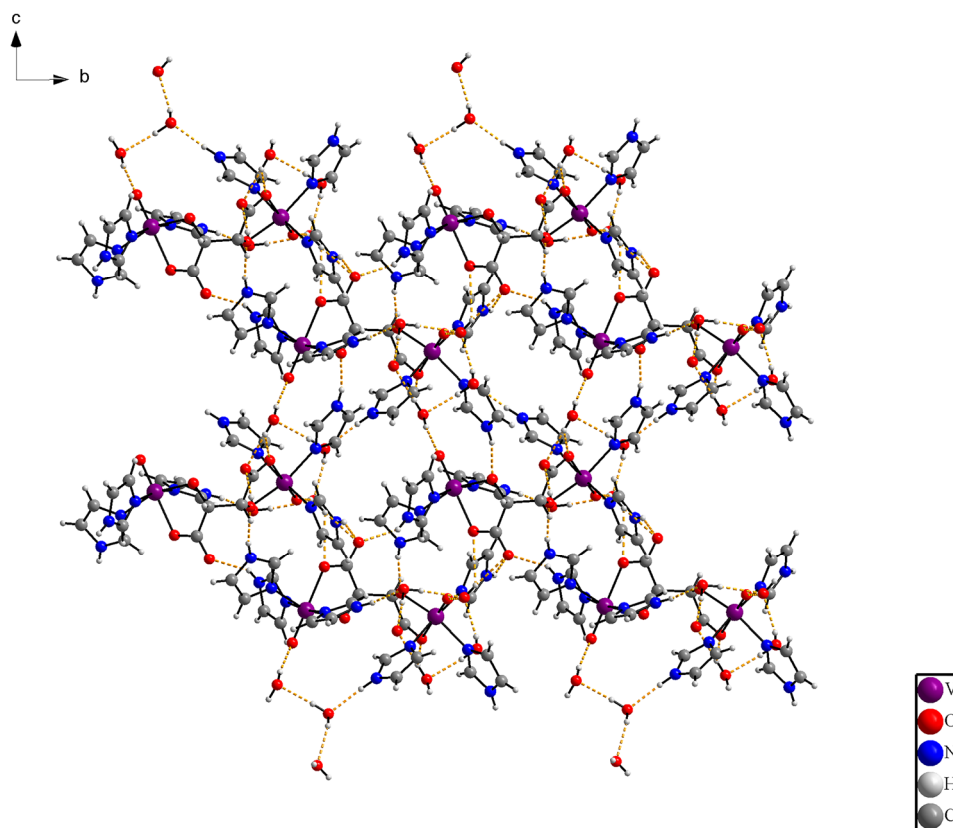


Figure S3. ORTEP plot of the anion structure $(\text{H}_2\text{im})_2[\Lambda,\Delta\text{-V}^{\text{IV}}\text{O}_2(\text{S,S-H}_2\text{tart})(\text{S,S-tart})(\text{Him})_2] \cdot \text{Him}$ (**3**) at the 30% probability levels.

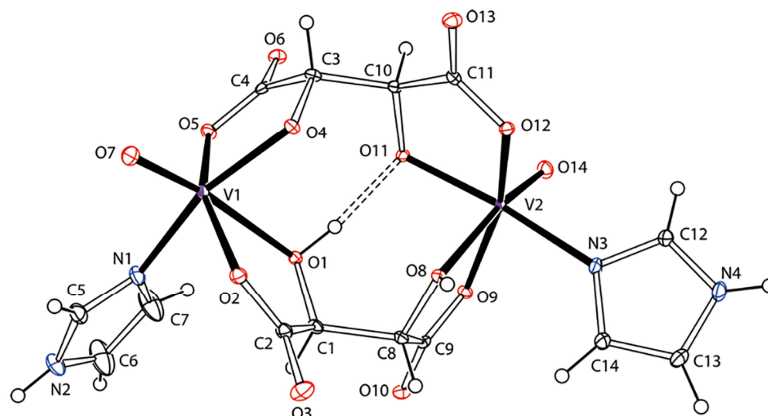


Figure S4. ORTEP plot of the molecular structure $[\Delta,\Delta\text{-V}^{\text{IV}}_2\text{O}_2(\text{S,S-tart})(\text{Him})_6]\cdot 4\text{H}_2\text{O}$ (**4**) at the 30% probability levels.

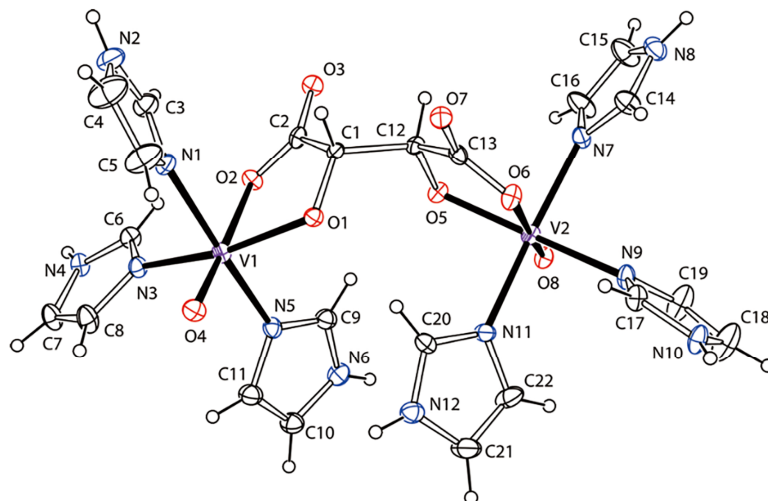


Figure S5. Chemdraw structures for oxidovanadium tartrates **5 – 8**, other oxidovanadium hydroxycarboxylates **9 – 16** and reported FeV-cos **17 – 21**.

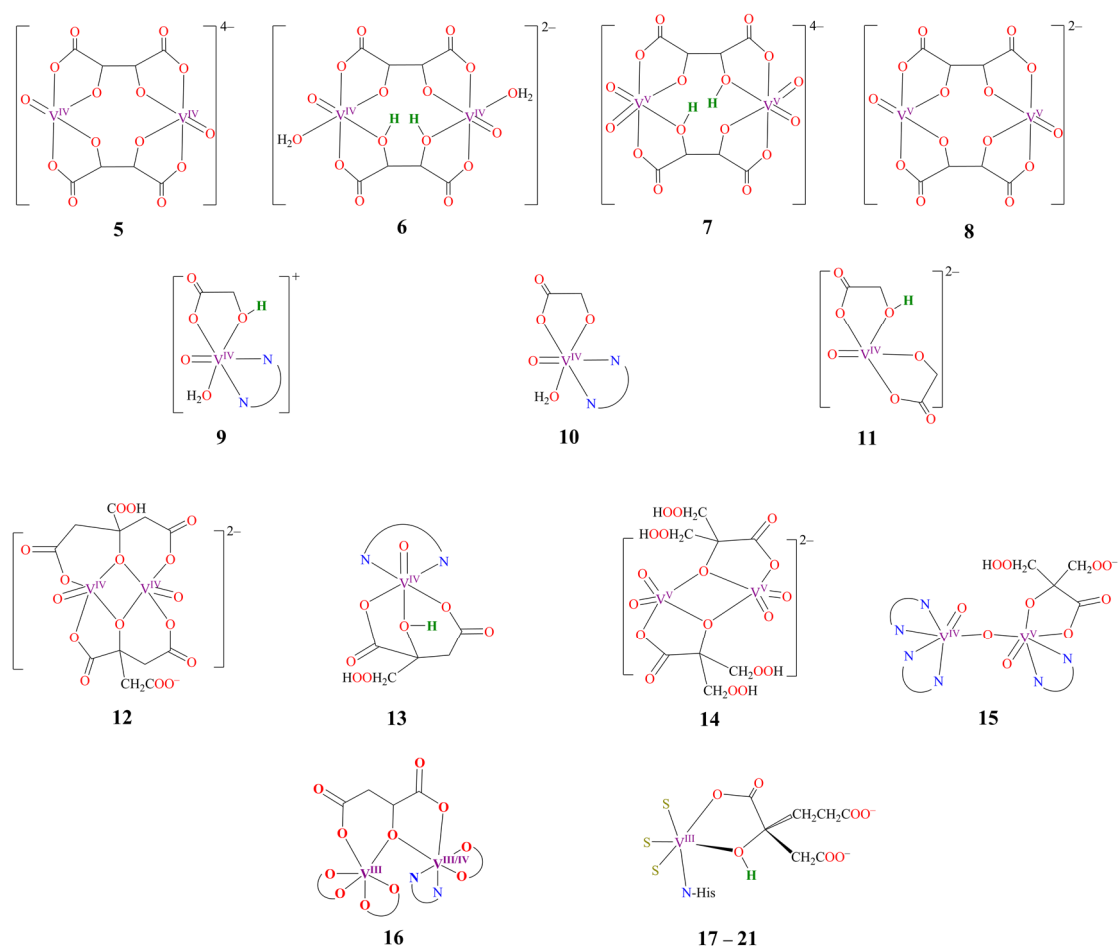


Figure S6. FT-IR spectrum of *R,R*-tartaric acid originated from Spectral Database for Organic Compounds SDBS. URL for this compound: <https://sdb.sdb.aist.go.jp/sdb/cgi-bin/landingpage?sdbno=1071>.

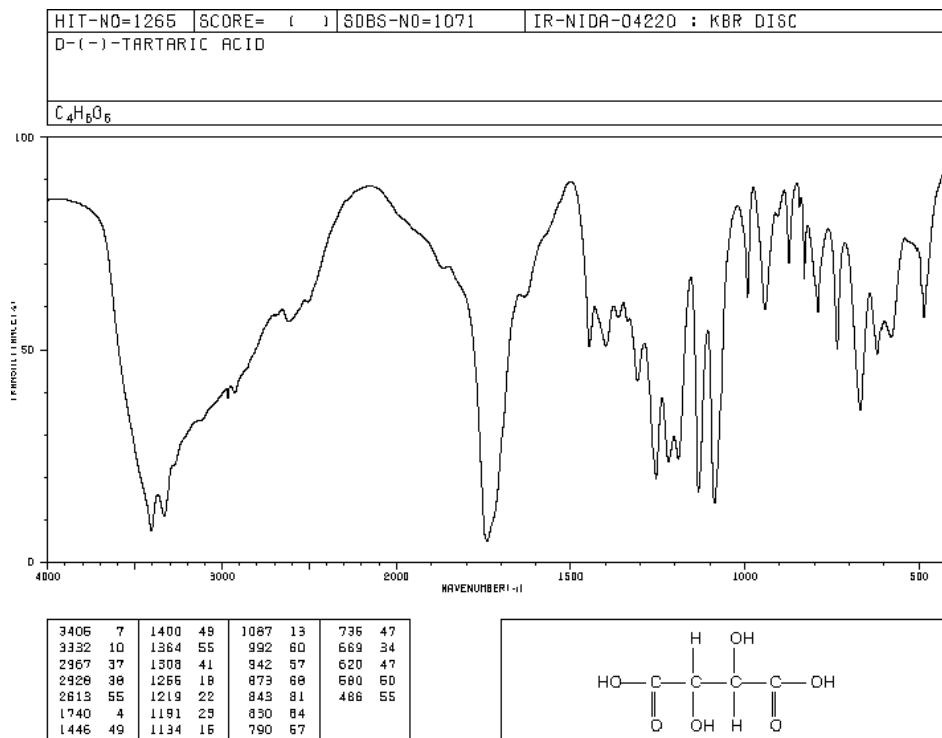


Figure S7. FT-IR spectrum of *S, S*-tartaric acid originated from Spectral Database for Organic Compounds SDBS. URL for this compound: <https://sdb.db.aist.go.jp/sdb/cgi-bin/landingpage?sdbno=488>.

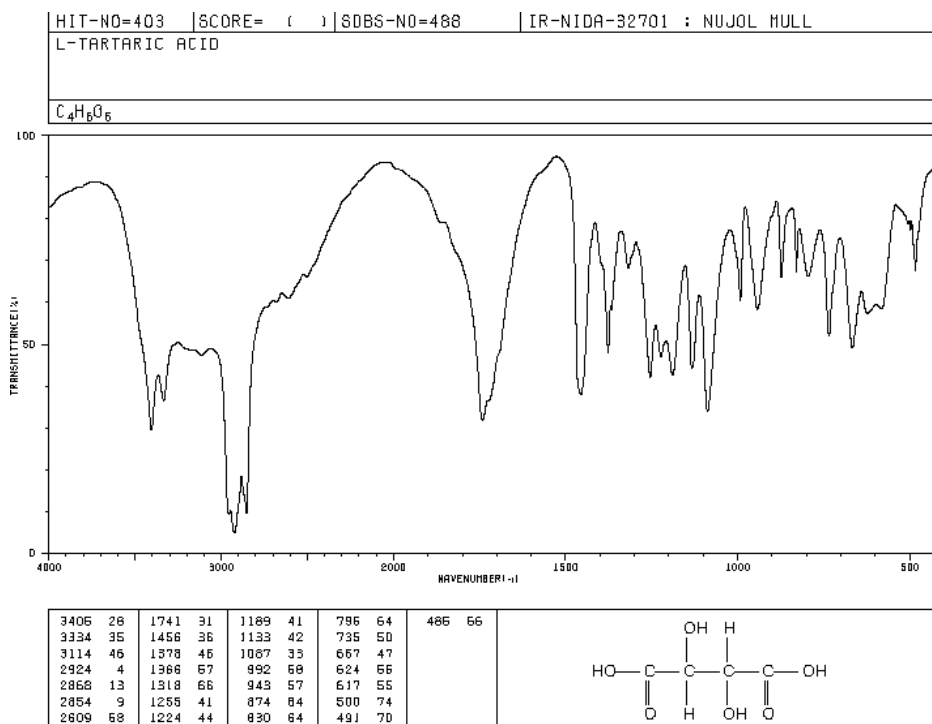


Figure S8a. VCD and IR spectra of $(\text{H}_2\text{im})_2[\Delta,\Lambda\text{-V}^{\text{IV}}_2\text{O}_2(\text{R,R-H}_2\text{tart})(\text{R,R-tart})(\text{Him})_2]\cdot\text{Him}$ (**1**) with KBr pellet.

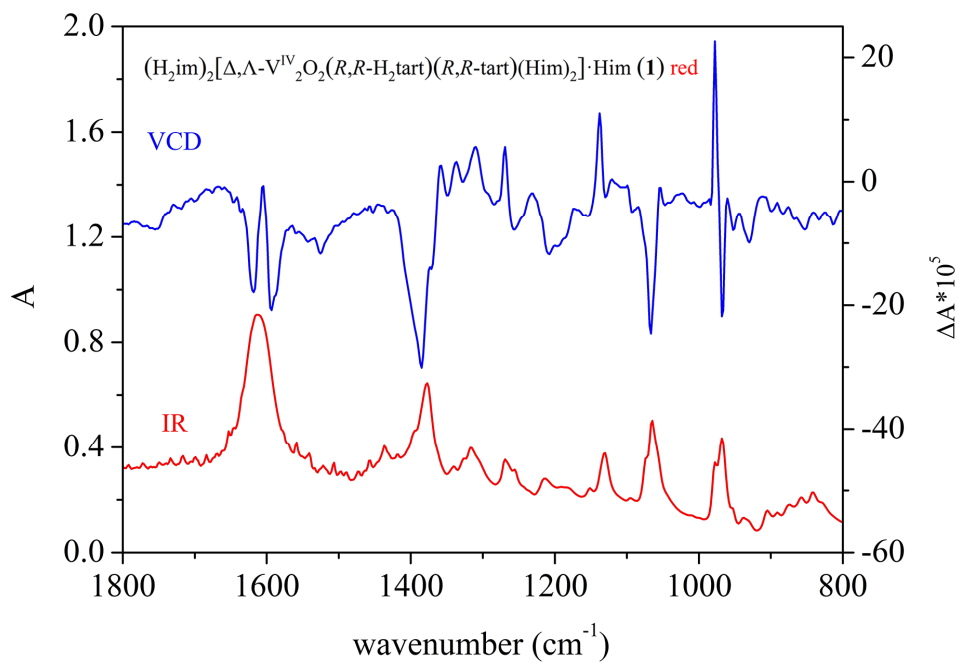


Figure S8b. VCD and IR spectra of $[\Lambda,\Lambda\text{-V}^{\text{IV}}_2\text{O}_2(R,R\text{-tart(Him)}_6)]\cdot 4\text{H}_2\text{O}$ (**2**) with KBr pellet.

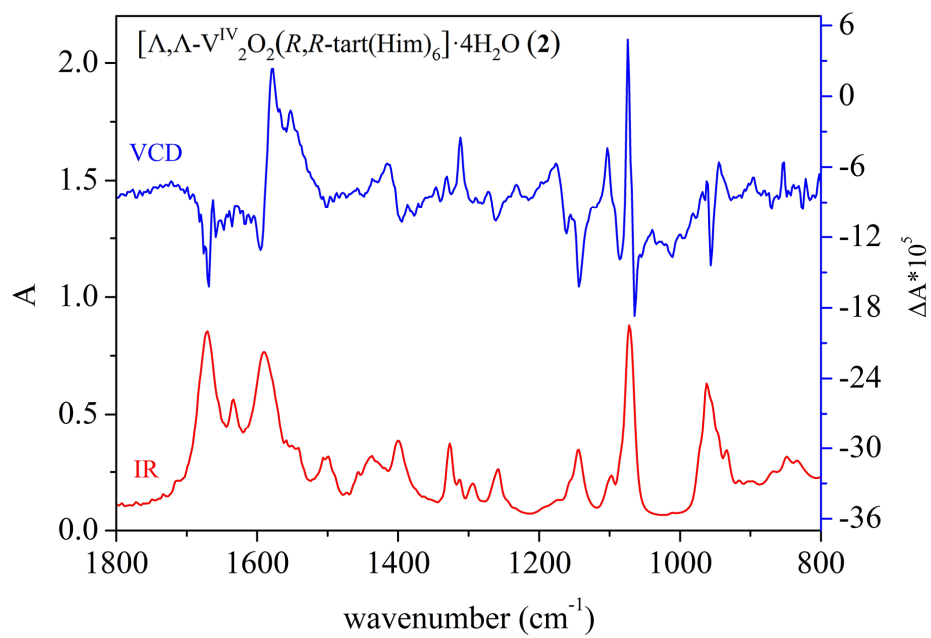


Figure S8c. VCD and IR spectra of $(\text{H}_2\text{im})_2[\Lambda,\Delta\text{-V}^{\text{IV}}\text{O}_2(\text{S,S-H}_2\text{tart})(\text{S,S-tart})(\text{Him})_2]\cdot\text{Him}$ (**3**) with KBr pellet.

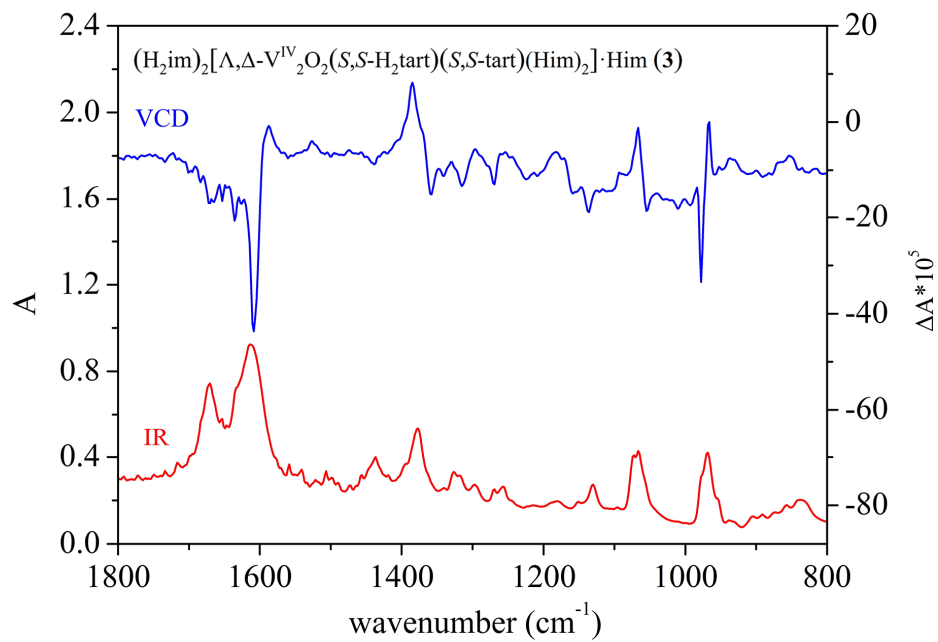


Figure S8d. VCD and IR spectra of $[\Delta,\Delta\text{-V}^{\text{IV}}_2\text{O}_2(\text{S,S-tart}(\text{Him})_6)]\cdot 4\text{H}_2\text{O}$ (**4**) with KBr pellet.

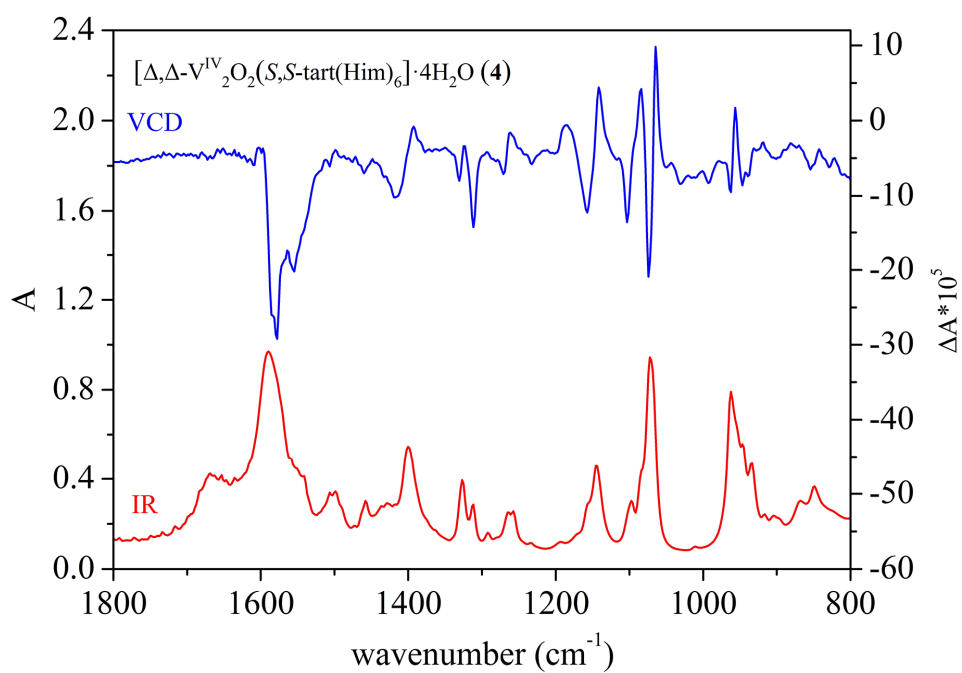


Figure S9. X-band EPR spectra of **1** and **3** in solid-states (a) and **1** in H₂O (b) at 298 K, respectively.

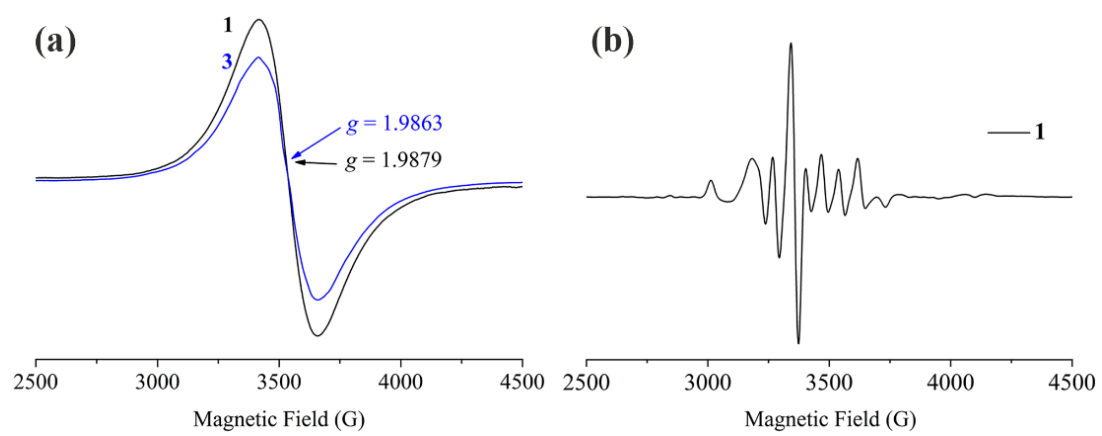


Figure S10. X-band EPR spectra with g -axis in solid state of **1** – **4** at 298 K, respectively.

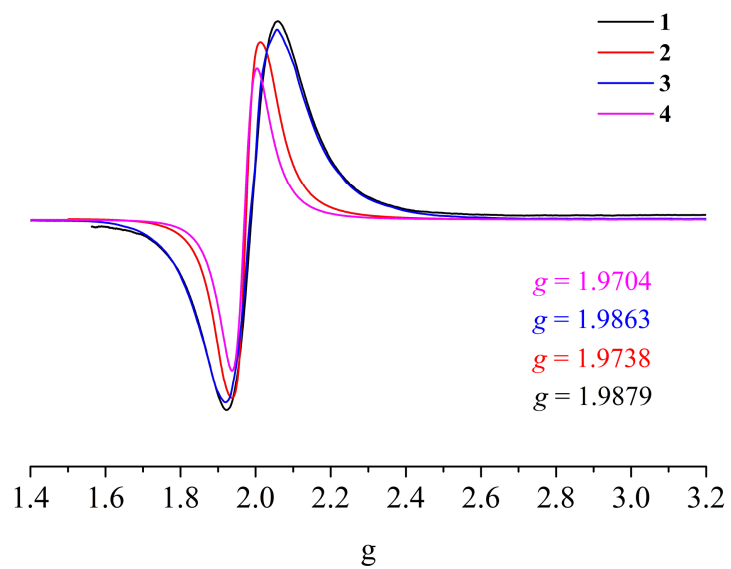


Figure S11. Temperature-dependence magnetic susceptibility of **2** in an applied field of $B = 0.1$ T over the range of 2 – 300 K. Red line correspond to the best fitting result.

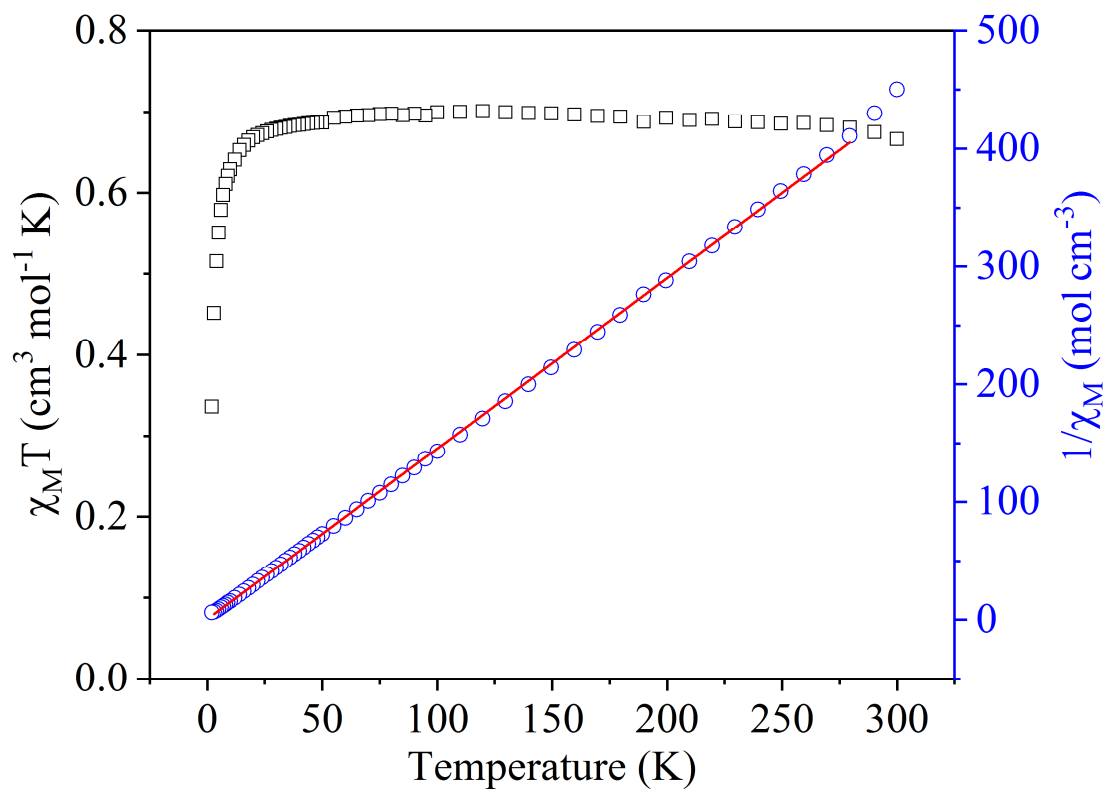


Figure S12. IR spectra of $(\text{H}_2\text{im})_2[\Delta,\Delta\text{-V}^{\text{IV}}_2\text{O}_2(\text{R,R-H}_2\text{tart})(\text{R,R-tart})(\text{Him})_2]\cdot\text{Him}$ (**1**), $[\Delta,\Delta\text{-V}^{\text{IV}}_2\text{O}_2(\text{R,R-tart})(\text{Him})_6]\cdot 4\text{H}_2\text{O}$ (**2**), $(\text{H}_2\text{im})_2[\Delta,\Delta\text{-V}^{\text{IV}}_2\text{O}_2(\text{S,S-H}_2\text{tart})(\text{S,S-tart})(\text{Him})_2]\cdot\text{Him}$ (**3**) and $[\Delta,\Delta\text{-V}^{\text{IV}}_2\text{O}_2(\text{S,S-tart})(\text{Him})_6]\cdot 4\text{H}_2\text{O}$ (**4**), respectively.

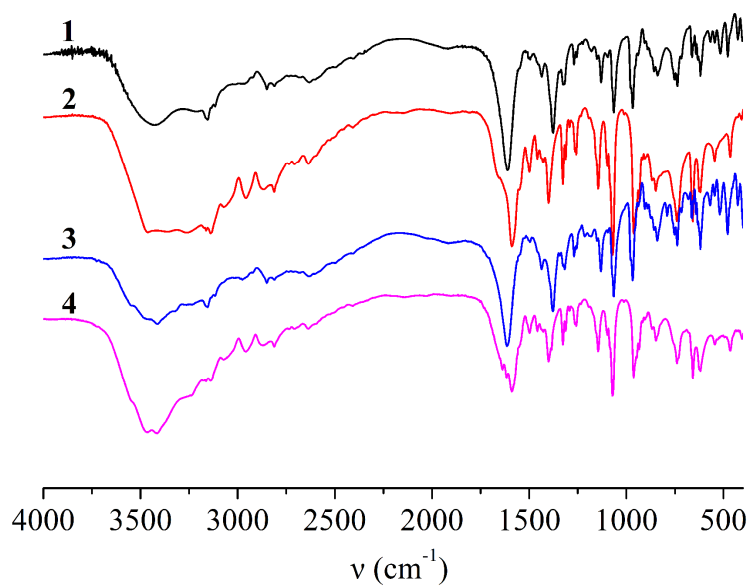


Figure S13. (a) Diffused reflectance UV-Vis spectra of solids $(\text{H}_2\text{im})_2[\Delta,\Lambda\text{-V}^{\text{IV}}_2\text{O}_2(\text{R,R-H}_2\text{tart})(\text{R,R-tart})(\text{Him})_2]\cdot\text{Him}$ (**1**), $[\Lambda,\Lambda\text{-V}^{\text{IV}}_2\text{O}_2(\text{R,R-tart})(\text{Him})_6]\cdot 4\text{H}_2\text{O}$ (**2**), $(\text{H}_2\text{im})_2[\Lambda,\Delta\text{-V}^{\text{IV}}_2\text{O}_2(\text{S,S-H}_2\text{tart})(\text{S,S-tart})(\text{Him})_2]\cdot\text{Him}$ (**3**) and $[\Delta,\Delta\text{-V}^{\text{IV}}_2\text{O}_2(\text{S,S-tart})(\text{Him})_6]\cdot 4\text{H}_2\text{O}$ (**4**), respectively. (b) Comparisons for solid and solution UV-Vis spectrum of $[\Lambda,\Lambda\text{-V}^{\text{IV}}_2\text{O}_2(\text{R,R-tart})(\text{Him})_6]\cdot 4\text{H}_2\text{O}$ (**2**) in water (inset: UV-Vis spectra with local amplification regions).

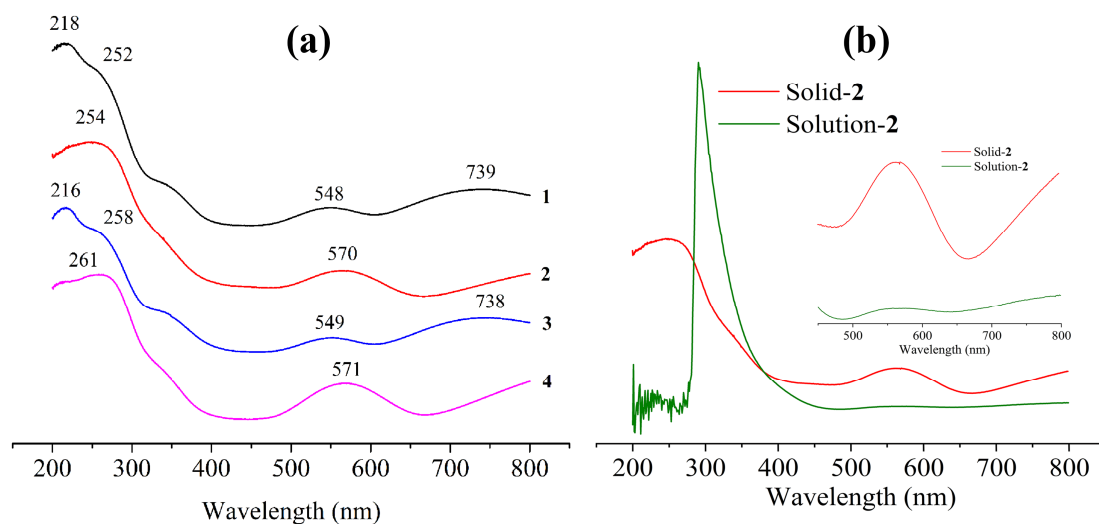


Figure S14. TG–DTG curves of $(\text{H}_2\text{im})_2[\Delta,\Lambda\text{-V}^{\text{IV}}\text{O}_2(\text{R,R-H}_2\text{tart})(\text{R,R-tart})(\text{Him})_2]\cdot\text{Him}$ (**1**, a); TG–DTG curves of $[\Lambda,\Lambda\text{-V}^{\text{IV}}\text{O}_2(\text{R,R-tart})(\text{Him})_6]\cdot 4\text{H}_2\text{O}$ (**2**, b); TG–DTG curves of $(\text{H}_2\text{im})_2[\Lambda,\Delta\text{-V}^{\text{IV}}\text{O}_2(\text{S,S-H}_2\text{tart})(\text{S,S-tart})(\text{Him})_2]\cdot\text{Him}$ (**3**, c); TG–DTG curves of $[\Delta,\Delta\text{-V}^{\text{IV}}\text{O}_2(\text{S,S-tart})(\text{Him})_6]\cdot 4\text{H}_2\text{O}$ (**4**, d).

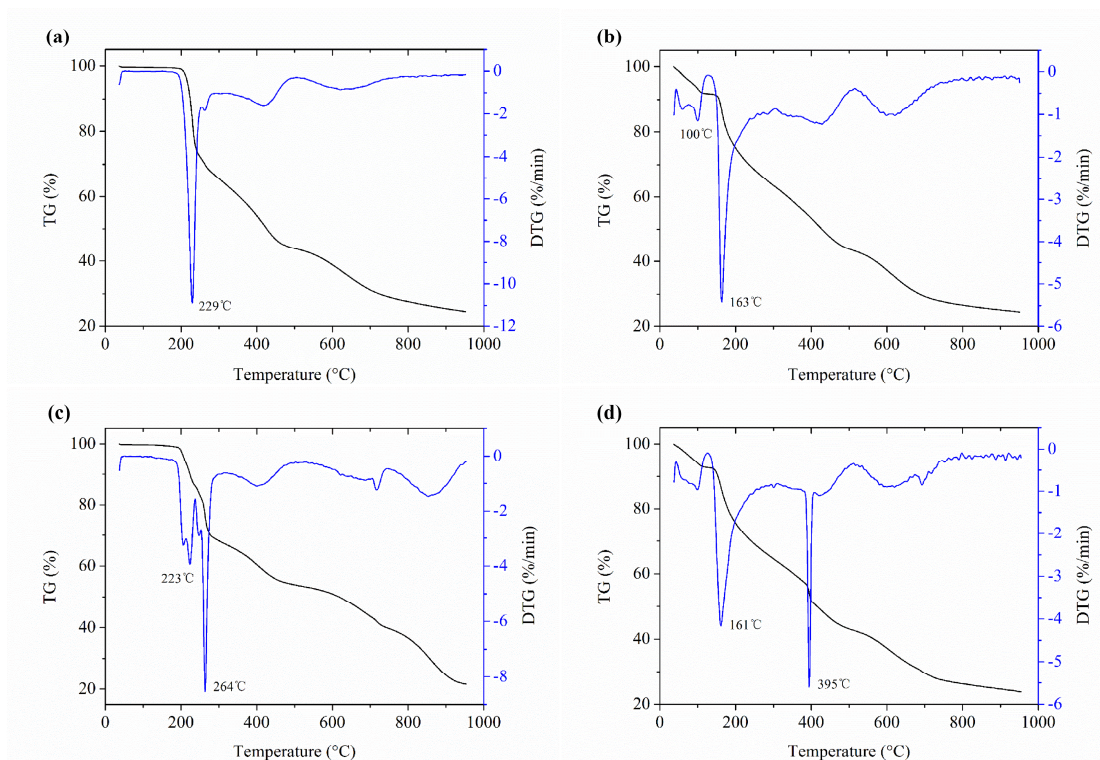


Figure S15. Cyclic voltammogram of $[\Lambda,\Lambda\text{-V}_2\text{O}_2(R,R\text{-tart})(\text{Him})_6]\cdot 4\text{H}_2\text{O}$ (**2**) in anhydrous DMF with 0.10 M $[\text{n-Bu}_4\text{N}]\text{ClO}_4$ at a glassy carbon electrode with scan rate of $50\text{ mV}\cdot\text{s}^{-1}$ (a) and various scan rates (b), respectively. (c) Plots of redox peak currents against $v^{1/2}$. (d) Differential pulse voltammogram of **2**.

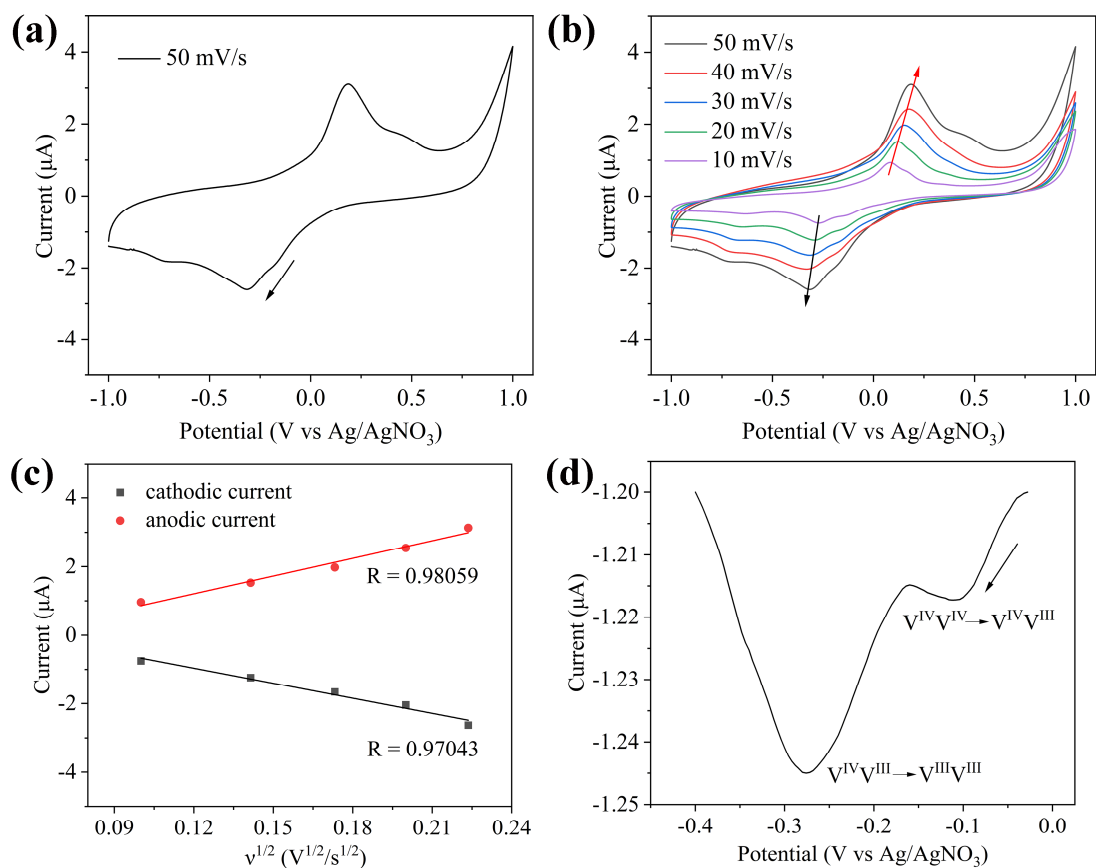


Figure S16. Comparison of the observed PXRD (red) with the simulated patterns (black) calculated from the crystal data for $[\Lambda,\Lambda\text{-V}^{\text{IV}}_2\text{O}_2(\text{R,R-tart})(\text{Him})_6]\cdot 4\text{H}_2\text{O}$ (**2**).

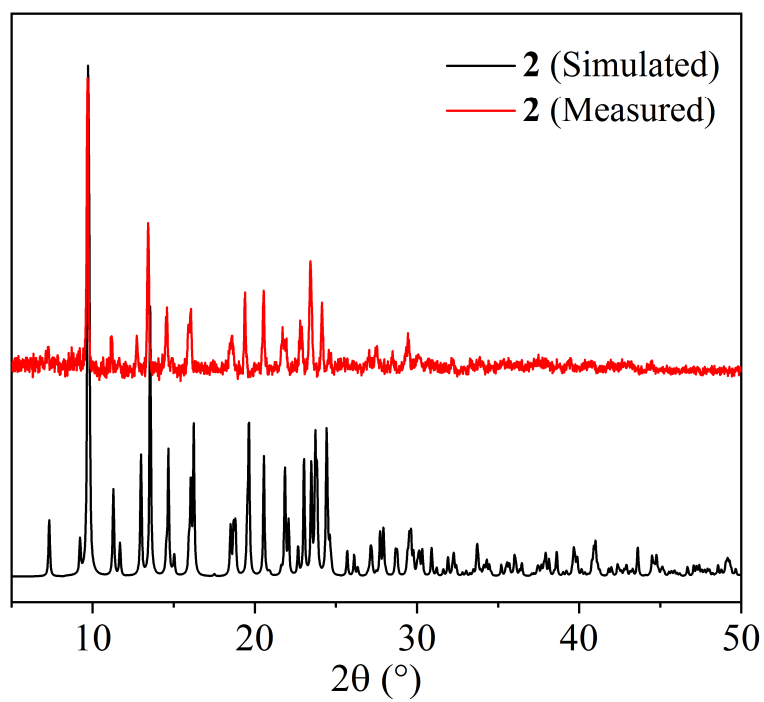


Table S1. Crystallographic data and structural refinements for complexes (H₂im)₂[Δ,Λ -V^{IV}O₂(*R,R*-H₂tart)(*R,R*-tart)(Him)₂] \cdot Him (**1**), [Λ,Λ -V^{IV}O₂(*R,R*-tart)(Him)₆] \cdot 4H₂O (**2**), (H₂im)₂[Λ,Δ -V^{IV}O₂(*S,S*-H₂tart)(*S,S*-tart)(Him)₂] \cdot Him (**3**) and [Δ,Δ -V^{IV}O₂(*S,S*-tart)(Him)₆] \cdot 4H₂O (**4**), respectively.

	1	2	3	4
Empirical formula	C ₂₃ H ₂₈ N ₁₀ O ₁₄ V ₂	C ₂₂ H ₃₄ N ₁₂ O ₁₂ V ₂	C ₂₃ H ₂₈ N ₁₀ O ₁₄ V ₂	C ₂₂ H ₃₄ N ₁₂ O ₁₂ V ₂
Formula weight	770.43	760.49	770.43	760.49
Temperature/K	173(1)	100(1)	100(1)	100(1)
Crystal system	monoclinic	monoclinic	monoclinic	monoclinic
Space group	<i>P</i> 2 ₁	<i>P</i> 2 ₁	<i>P</i> 2 ₁	<i>P</i> 2 ₁
<i>a</i> /Å	8.9068(3)	10.1662(1)	8.8863(1)	10.1454(2)
<i>b</i> /Å	19.6606(6)	13.6125(1)	19.5997(1)	13.6326(2)
<i>c</i> /Å	9.8849(4)	12.8047(1)	9.8686(1)	12.7784(2)
α /°	90	90	90	90
β /°	109.160(4)	109.405(1)	108.907(1)	109.196(2)
γ /°	90	90	90	90
Volume/Å ³	1635.1(1)	1671.35(3)	1626.07(3)	1669.09(5)
<i>Z</i>	2	2	2	2
ρ_{calc} /cm ³	1.565	1.511	1.574	1.513
μ /mm ⁻¹	0.652	5.352	5.544	5.359
<i>F</i> (000)	788	784	788	784
Crystal size/mm ³	0.4 \times 0.3 \times 0.2	0.1 \times 0.1 \times 0.1	0.2 \times 0.2 \times 0.2	0.2 \times 0.15 \times 0.15
Radiation	MoK α (λ = 0.71073)	CuK α (λ = 1.54184)	CuK α (λ = 1.54184)	CuK α (λ = 1.54184)

2θ range for data collection/ $^{\circ}$	4.362 to 49.98	7.32 to 155.708	9.474 to 155.064	7.326 to 156.334
Reflections collected	5991	22233	16285	11514
Independent reflections	4595	6846	4870	5339
R_{int}	0.0298	0.0301	0.0249	0.0318
Data/restraints/parameters	4595/188/472	6846/2/469	4870/16/449	5339/26/469
Goodness of fit on F^2	1.043	1.036	1.083	1.161
Final R indexes [$I \geq 2\sigma(I)$]	$R_1 = 0.0377$, $wR_2 = 0.0904$	$R_1 = 0.0257$, $wR_2 = 0.0662$	$R_1 = 0.0266$, $wR_2 = 0.0698$	$R_1 = 0.0384$, $wR_2 = 0.1091$
Final R indexes [all data]	$R_1 = 0.0405$, $wR_2 = 0.0932$	$R_1 = 0.0300$, $wR_2 = 0.0695$	$R_1 = 0.0289$, $wR_2 = 0.0713$	$R_1 = 0.0481$, $wR_2 = 0.1233$
Largest diff. peak/hole / $e \text{ \AA}^{-3}$	0.40/-0.36	0.23/-0.39	0.24/-0.53	0.74/-0.74
Flack parameter	0.02(2)	-0.002(2)	0.009(3)	0.005(5)

Table S2. Selected hydrogen bonds (Å) in (H₂im)₂[Δ,Λ-V^{IV}₂O₂(*R,R*-H₂tart)(*R,R*-tart)(Him)₂]·Him (**1**).

Donor–H···Acceptor	D–H(Å)	H···A(Å)	D···A(Å)	D–H···A(°)
O(4)–H(4)···N(9)	0.86(3)	1.69(2)	2.530(6)	169(4)
O(11)–H(11)···O(1)	0.88(2)	1.92(2)	2.731(5)	153(3)
N(2)–H(2)···O(13) ^a	0.88	1.82	2.695(7)	175
N(4)–H(4A)···O(5) ^b	0.79(9)	2.08(8)	2.836(7)	160(8)
N(5)–H(5A)···O(1)	0.88	1.89	2.755(5)	167
N(6)–H(6A)···O(2) ^c	0.88	2.54	3.093(5)	121
N(6)–H(6A)···O(3) ^c	0.88	2.02	2.876(6)	163
N(7)–H(7A)···O(8)	0.98(8)	1.60(7)	2.573(6)	175(9)
N(8)–H(8A)···O(10) ^d	0.80(6)	1.94(6)	2.723(6)	167(6)
N(10)–H(10A)···O(6) ^d	0.88	1.95	2.811(6)	166

Symmetric codes: (a) $2 - x, \frac{1}{2} + y, 1 - z$; (b) $2 - x, -\frac{1}{2} + y, 2 - z$; (c) $x, y, 1 + z$; (d) $x, y, -1 + z$.

Table S3. Selected hydrogen bonds (Å) in $[\Lambda, \Lambda\text{-V}^{\text{IV}}_2\text{O}_2(R,R\text{-tart})(\text{Him})_6] \cdot 4\text{H}_2\text{O}$ (**2**).

Donor–H \cdots Acceptor	D–H(Å)	H \cdots A(Å)	D \cdots A(Å)	D–H \cdots A(°)
O(1w)–H(1wA) \cdots O(7)	0.84(5)	1.88(5)	2.719(3)	176(6)
O(1w)–H(1wB) \cdots O(2w) ^a	0.84(7)	2.05(7)	2.886(4)	174(5)
O(2w)–H(2wA) \cdots O(2) ^b	0.76(5)	2.56(5)	3.104(3)	131(5)
O(2w)–H(2wA) \cdots O(3) ^b	0.76(5)	2.14(5)	2.889(3)	172(5)
O(2w)–H(2wB) \cdots O(8) ^c	0.75(5)	1.96(5)	2.697(4)	171(5)
O(3w)–H(3wA) \cdots O(2w)	0.82(6)	2.01(6)	2.767(4)	153(6)
O(3w)–H(3wB) \cdots O(4w)	0.85(3)	1.88(4)	2.703(4)	162(6)
O(4w)–H(4wB) \cdots O(4)	0.83(5)	1.98(5)	2.803(3)	172(5)
O(4w)–H(4wA) \cdots O(7) ^d	0.87(5)	1.88(5)	2.741(3)	170(5)
N(2)–H(2) \cdots O(3) ^e	0.86(5)	2.10(4)	2.885(4)	151(4)
N(4)–H(4) \cdots O(5) ^f	0.86	1.93	2.778(3)	168
N(6)–H(6) \cdots O(1w) ^g	0.86	1.97	2.816(4)	169
N(8)–H(8) \cdots O(3) ^h	0.86	2.03	2.822(4)	153
N(10)–H(10) \cdots O(1)	0.86	1.92	2.756(3)	165
N(12)–H(12) \cdots O(3w)	0.86	1.86	2.722(4)	176

Symmetric codes: (a) $1 - x, \frac{1}{2} + y, 1 - z$; (b) $x, y, 1 + z$; (c) $-x, -\frac{1}{2} + y, 1 - z$; (d) $1 - x, -\frac{1}{2} + y, 1 - z$; (e) $1 - x, -\frac{1}{2} + y, -z$; (f) $-x, -\frac{1}{2} + y, -z$; (g) $-1 + x, y, z$; (h) $1 - x, \frac{1}{2} + y, -z$.

Table S4. Selected hydrogen bonds (Å) in (H₂im)₂[Λ,Δ-V^{IV}O₂(S,S-H₂tart)(S,S-tart)(Him)₂]·Him (**3**).

Donor–H⋯Acceptor	D–H(Å)	H⋯A(Å)	D⋯A(Å)	D–H⋯A(°)
O(1)–H(1)⋯O(4)	0.90(5)	2.49(5)	2.802(2)	101(4)
O(1)–H(1)⋯O(8)	0.90(5)	2.34(5)	2.812(3)	112(4)
O(1)–H(1)⋯O(11)	0.90(5)	1.85(6)	2.724(3)	163(4)
N(2)–H(2)⋯O(9) ^a	0.86	2.01	2.819(4)	157
N(4)–H(4)⋯O(3) ^b	0.86	1.83	2.686(4)	174
N(5)–H(5A)⋯O(4)	0.86	1.75	2.565(3)	158
N(6)–H(6A)⋯O(6) ^c	0.86	1.9	2.720(3)	158
N(7)–H(7A)⋯O(11)	0.86	1.9	2.742(3)	166
O(8)–H(8)⋯N(9)	0.87(2)	1.65(2)	2.509(3)	171(3)
N(8)–H(8B)⋯O(12) ^d	0.86	2.55	3.085(3)	121
N(8)–H(8B)⋯O(13) ^d	0.86	2.01	2.837(3)	163
N(10)–H(10A)⋯O(10) ^c	0.86	1.96	2.796(3)	166

Symmetric codes: (a) $2 - x, \frac{1}{2} + y, 2 - z$; (b) $2 - x, -\frac{1}{2} + y, 1 - z$; (c) $x, y, -1 + z$; (d) $x, y, 1 + z$.

Table S5. Selected hydrogen bonds (Å) in $[\Delta,\Delta\text{-V}^{\text{IV}}_2\text{O}_2(\text{S,S-tart})(\text{Him})_6]\cdot 4\text{H}_2\text{O}$ (**4**).

Donor–H \cdots Acceptor	D–H(Å)	H \cdots A(Å)	D \cdots A(Å)	D–H \cdots A(°)
O(2w)–H(2wA) \cdots O(3) ^a	0.81(7)	1.91(7)	2.723(6)	175(7)
N(2)–H(2) \cdots O(3) ^b	0.86	2.02	2.817(8)	153
O(1w)–H(1wA) \cdots O(4)	0.85(1)	1.85(1)	2.687(8)	172(9)
O(2w)–H(2wB) \cdots O(1w)	0.85(1)	2.04(1)	2.877(10)	172(1)
N(4)–H(4) \cdots O(5) ^c	0.86	1.92	2.759(6)	163
O(1w)–H(1wB) \cdots O(7) ^d	0.68(1)	2.22(1)	2.895(8)	170(1)
O(4w)–H(4wA) \cdots O(1w) ^e	0.87(7)	1.95(7)	2.759(9)	154(7)
N(6)–H(6) \cdots O(4w)	0.86	1.85	2.709(9)	175
O(4w)–H(4wB) \cdots O(3w)	0.85(7)	1.86(7)	2.694(9)	168(1)
O(3w)–H(3wA) \cdots O(3) ^f	0.80(1)	1.95(1)	2.739(7)	168(7)
N(8)–H(8) \cdots O(7) ^g	0.86	2.12	2.878(8)	148
O(3w)–H(3wB) \cdots O(8)	0.86(7)	1.95(7)	2.795(7)	171(7)
N(10)–H(10) \cdots O(1) ^h	0.76(1)	2.03(1)	2.780(7)	172(1)
N(12)–H(12) \cdots O(2w)	0.86	1.96	2.809(9)	169

Symmetric codes: (a) $1 + x, y, z$; (b) $-x, -\frac{1}{2} + y, 2 - z$; (c) $-x, -\frac{1}{2} + y, 1 - z$; (d) $1 - x, -\frac{1}{2} + y, 2 - z$; (e) $1 - x, \frac{1}{2} + y, 1 - z$; (f) $-x, \frac{1}{2} + y, 1 - z$; (g) $-x, \frac{1}{2} + y, 2 - z$; (h) $1 - x, \frac{1}{2} + y, 2 - z$.

Table S6. Selected bond distances (Å) and angles (°) for (H₂im)₂[Δ,Λ-V^{IV}O₂(*R,R*-H₂tart)(*R,R*-tart)(Him)₂] \cdot Him (**1**).

1			
V(1)–O(1)	1.989(3)	V(2)–O(8)	1.961(3)
V(1)–O(2)	1.987(3)	V(2)–O(9)	1.990(4)
V(1)–O(4)	2.155(3)	V(2)–O(11)	2.318(3)
V(1)–O(5)	2.051(3)	V(2)–O(12)	2.007(3)
V(1)–O(7)	1.603(4)	V(2)–O(14)	1.595(4)
V(1)–N(1)	2.130(4)	V(2)–N(3)	2.126(4)
O(1)–V(1)–O(5)	90.1(1)	O(8)–V(2)–O(11)	81.5(1)
O(1)–V(1)–O(4)	84.9(1)	O(8)–V(2)–O(9)	81.4(1)
O(1)–V(1)–N(1)	166.2(2)	O(8)–V(2)–O(12)	90.4(2)
O(2)–V(1)–O(5)	159.3(1)	O(8)–V(2)–N(3)	161.0(2)
O(2)–V(1)–O(4)	85.6(1)	O(9)–V(2)–O(11)	81.0(1)
O(2)–V(1)–O(1)	82.0(1)	O(9)–V(2)–O(12)	155.6(2)
O(2)–V(1)–N(1)	91.3(2)	O(9)–V(2)–N(3)	91.7(2)
O(5)–V(1)–O(4)	74.7(1)	O(12)–V(2)–O(11)	75.0(1)
O(5)–V(1)–N(1)	92.1(2)	O(12)–V(2)–N(3)	88.7(2)
O(7)–V(1)–O(2)	105.4(2)	O(14)–V(2)–O(11)	171.5(2)
O(7)–V(1)–O(5)	94.8(2)	O(14)–V(2)–O(8)	103.9(2)
O(7)–V(1)–O(4)	168.4(2)	O(14)–V(2)–O(9)	106.1(2)
O(7)–V(1)–O(1)	100.2(2)	O(14)–V(2)–O(12)	98.2(2)
O(7)–V(1)–N(1)	93.3(2)	O(14)–V(2)–N(3)	95.0(2)
N(1)–V(1)–O(4)	82.5(2)	N(3)–V(2)–O(11)	79.9(2)

Table S7. Selected bond distances (Å) and angles (°) for $[\Lambda,\Lambda\text{-V}^{\text{IV}}_2\text{O}_2(R,R\text{-tart})(\text{Him})_6]\cdot 4\text{H}_2\text{O}$ (**2**).

2			
V(1)–O(1)	1.975(2)	V(2)–O(5)	1.976(2)
V(1)–O(2)	2.159(2)	V(2)–O(6)	2.112(2)
V(1)–O(4)	1.608(2)	V(2)–O(8)	1.618(2)
V(1)–N(1)	2.143(2)	V(2)–N(7)	2.122(2)
V(1)–N(3)	2.111(2)	V(2)–N(9)	2.102(2)
V(1)–N(5)	2.118(3)	V(2)–N(11)	2.103(2)
O(1)–V(1)–O(2)	77.61(8)	O(5)–V(2)–O(6)	78.43(8)
O(1)–V(1)–N(3)	160.48(9)	O(5)–V(2)–N(9)	161.11(9)
O(1)–V(1)–N(1)	92.24(9)	O(5)–V(2)–N(11)	92.22(9)
O(1)–V(1)–N(5)	90.52(9)	O(5)–V(2)–N(7)	89.43(9)
O(4)–V(1)–O(1)	101.77(9)	O(6)–V(2)–N(7)	85.11(9)
O(4)–V(1)–O(2)	178.0(1)	O(8)–V(2)–O(6)	177.9(1)
O(4)–V(1)–N(3)	97.5(1)	O(8)–V(2)–O(5)	102.32(9)
O(4)–V(1)–N(1)	92.6(1)	O(8)–V(2)–N(9)	96.6(1)
O(4)–V(1)–N(5)	94.8(1)	O(8)–V(2)–N(11)	94.8(1)
N(3)–V(1)–O(2)	83.22(9)	O(8)–V(2)–N(7)	93.0(1)
N(3)–V(1)–N(1)	89.9(1)	N(9)–V(2)–O(6)	82.74(9)
N(3)–V(1)–N(5)	84.9(1)	N(9)–V(2)–N(11)	85.4(1)
N(1)–V(1)–O(2)	85.56(9)	N(9)–V(2)–N(7)	90.4(1)
N(5)–V(1)–O(2)	87.15(9)	N(11)–V(2)–O(6)	87.12(9)
N(5)–V(1)–N(1)	171.47(9)	N(11)–V(2)–N(7)	171.6(1)

Table S8. Selected bond distances (Å) and angles (°) for (H₂im)₂[Λ,Δ-V^{IV}₂O₂(S,S-H₂tart)(S,S-tart)(Him)₂]·Him (**3**).

3			
V(1)–O(1)	2.314(2)	V(2)–O(8)	1.991(2)
V(1)–O(2)	2.011(2)	V(2)–O(9)	2.056(2)
V(1)–O(4)	1.964(2)	V(2)–O(11)	2.146(2)
V(1)–O(5)	1.994(2)	V(2)–O(12)	1.995(2)
V(1)–O(7)	1.603(2)	V(2)–O(14)	1.605(2)
V(1)–N(1)	2.118(2)	V(2)–N(3)	2.129(2)
O(2)–V(1)–O(1)	75.12(7)	O(9)–V(2)–O(8)	75.21(7)
O(2)–V(1)–N(1)	88.53(9)	O(9)–V(2)–N(3)	92.42(8)
O(4)–V(1)–O(1)	81.39(7)	O(11)–V(2)–O(9)	90.11(7)
O(4)–V(1)–O(5)	81.26(8)	O(11)–V(2)–O(8)	85.02(7)
O(4)–V(1)–O(2)	90.30(8)	O(11)–V(2)–N(3)	165.89(9)
O(4)–V(1)–N(1)	160.38(9)	O(12)–V(2)–O(9)	159.71(8)
O(5)–V(1)–O(1)	80.85(7)	O(12)–V(2)–O(8)	85.51(7)
O(5)–V(1)–O(2)	155.48(8)	O(12)–V(2)–O(11)	81.88(7)
O(5)–V(1)–N(1)	91.83(9)	O(12)–V(2)–N(3)	91.13(8)
O(7)–V(1)–O(1)	171.50(9)	O(14)–V(2)–O(12)	105.32(9)
O(7)–V(1)–O(4)	104.04(9)	O(14)–V(2)–O(9)	94.38(9)
O(7)–V(1)–O(5)	106.3(1)	O(14)–V(2)–O(8)	168.53(9)
O(7)–V(1)–O(2)	98.1(1)	O(14)–V(2)–O(11)	100.02(9)
O(7)–V(1)–N(1)	95.5(1)	O(14)–V(2)–N(3)	93.6(1)
N(1)–V(1)–O(1)	79.39(9)	N(3)–V(2)–O(8)	82.21(9)

Table S9. Selected bond distances (Å) and angles (°) for [Δ,Δ -V^{IV}₂O₂(*S,S*-tart)(Him)₆] \cdot 4H₂O (**4**).

4			
V(1)–O(1)	1.977(4)	V(2)–O(5)	1.966(4)
V(1)–O(2)	2.114(4)	V(2)–O(6)	2.160(4)
V(1)–O(4)	1.615(4)	V(2)–O(8)	1.596(4)
V(1)–N(1)	2.127(5)	V(2)–N(7)	2.148(5)
V(1)–N(3)	2.091(5)	V(2)–N(9)	2.125(5)
V(1)–N(5)	2.105(5)	V(2)–N(11)	2.126(5)
O(1)–V(1)–O(2)	78.3(2)	O(5)–V(2)–O(6)	77.6(2)
O(1)–V(1)–N(3)	161.2(2)	O(5)–V(2)–N(7)	92.2(2)
O(1)–V(1)–N(5)	92.4(2)	O(5)–V(2)–N(9)	160.7(2)
O(1)–V(1)–N(1)	89.6(2)	O(5)–V(2)–N(11)	90.6(2)
O(2)–V(1)–N(1)	85.3(2)	O(8)–V(2)–O(5)	101.56(2)
O(4)–V(1)–O(2)	178.1(2)	O(8)–V(2)–O(6)	178.0(2)
O(4)–V(1)–O(1)	102.3(2)	O(8)–V(2)–N(7)	92.7(2)
O(4)–V(1)–N(3)	96.4(2)	O(8)–V(2)–N(9)	97.5(2)
O(4)–V(1)–N(5)	95.0(2)	O(8)–V(2)–N(11)	94.5(2)
O(4)–V(1)–N(1)	92.9(2)	N(7)–V(2)–O(6)	85.6(2)
N(3)–V(1)–O(2)	82.9(2)	N(9)–V(2)–O(6)	83.4(2)
N(3)–V(1)–N(5)	85.5(2)	N(9)–V(2)–N(7)	90.0(2)
N(3)–V(1)–N(1)	89.9(2)	N(9)–V(2)–N(11)	84.7(2)
N(5)–V(1)–O(2)	86.8(2)	N(11)–V(2)–O(6)	87.3(2)
N(5)–V(1)–N(1)	171.3(2)	N(11)–V(2)–N(7)	171.6(2)

Table S10a. The formulas of oxidovanadium tartrates **1** – **18**, other oxidovanadium hydroxycarboxylates **19** – **38** and reported FeV-cos **39** – **43**.

Complexes (V ⁿ⁺)	Formulas
1 (+4)	(H ₂ im) ₂ [Δ,Λ-V ^{IV} ₂ O ₂ (<i>R,R</i> -H ₂ tart)(<i>R,R</i> -tart)(Him) ₂]·Him
2 (+4)	[Λ,Λ-V ^{IV} ₂ O ₂ (<i>R,R</i> -tart)(Him) ₆]·4H ₂ O
3 (+4)	(H ₂ im) ₂ [Λ,Δ-V ^{IV} ₂ O ₂ (<i>S,S</i> -H ₂ tart)(<i>S,S</i> -tart)(Him) ₂]·Him
4 (+4)	[Δ,Δ-V ^{IV} ₂ O ₂ (<i>S,S</i> -tart)(Him) ₆]·4H ₂ O
5 ¹ (+4)	(NH ₄) ₄ [V ₂ O ₂ (tart) ₂]·2H ₂ O
6 ² (+4)	Na ₄ [V ₂ O ₂ (tart) ₂]·12H ₂ O
7 ³ (+4)	Rb ₄ [V ₂ O ₂ (tart) ₂]·2H ₂ O
8 ³ (+4)	Cs ₄ [V ₂ O ₂ (tart) ₂]·2H ₂ O
9 ⁴ (+4)	Ca ₂ [V ₂ O ₂ (tart) ₂]·8H ₂ O
10 ⁵ (+4)	(NEt ₄) ₄ [V ₂ O ₂ (tart) ₂]·8H ₂ O
11 ⁶ (+4)	Cs ₂ [V ₂ O ₂ (H ₂ tart)(tart)(H ₂ O) ₂]·2H ₂ O
12 ⁶ (+4)	Rb ₂ [V ₂ O ₂ (H ₂ tart)(tart)(H ₂ O) ₂]·2H ₂ O
13 ⁶ (+4)	K ₂ [(VO) ₂ (tart) ₂ (H ₂ O) ₂]·2H ₂ O
14 ⁶ (+4)	[Na ₂ (H ₂ O) ₅ V ₂ O ₂ (H ₂ tart)(tart)]·2H ₂ O
15 ⁷ (+4)	[VO(O ₂)(bpz*eaT)·VO(H ₂ tart)]·H ₂ O
16 ⁸ (+5)	(NMe ₄) ₂ [V ₂ O ₄ (<i>R,R</i> -H ₂ tart) ₂]·6H ₂ O
17 ⁸ (+5)	(NMe ₄) ₂ [V ₂ O ₂ (<i>R,R</i> -tart)(<i>S,S</i> -tart)]
18 ⁸ (+5)	(NEt ₄) ₂ [V ₂ O ₂ (<i>R,R</i> -tart)(<i>S,S</i> -tart)]
19 ⁹ (+4)	[VO(Hglyc)(phen)(H ₂ O)]Cl·2H ₂ O
20 ⁹ (+4)	[VO(glyc)(bpy)(H ₂ O)]
21 ⁹ (+4)	(NH ₄) ₂ [VO(glyc)(Hglyc) ₂]·H ₂ O
22 ¹⁰ (+4)	K ₃ [V ₂ O ₂ (Hcit)(cit)]·7H ₂ O
23 ¹⁰ (+4)	Na ₄ [V ₂ O ₂ (cit) ₂]·12H ₂ O
24 ¹⁰ (+4)	(NH ₄) ₄ [V ₂ O ₂ (cit) ₂]·2H ₂ O
25 ¹¹ (+4)	[VO(H ₂ cit)(bpy)]·2H ₂ O
26 ¹¹ (+4)	[VO(H ₂ cit)(phen)]·1.5H ₂ O
27 ¹¹ (+4)	[VO(H ₂ cit)(phen)] ₂ ·6.5H ₂ O
28 ¹² (+4)	[VO(H ₂ cit)(bpy)]·1.5H ₂ O
29 ¹³ (+5)	Na ₂ [V ₂ O ₄ (H ₂ cit) ₂]·2H ₂ O
30 ¹⁴ (+5)	(NH ₄) ₄ [V ₂ O ₄ (Hcit) ₂]·4H ₂ O
31 ¹⁴ (+5)	(NH ₄) ₆ [V ₂ O ₄ (cit) ₂]·6H ₂ O
32 ¹⁵ (+5)	[V ₂ O ₃ (phen) ₃ (Hcit)]·5H ₂ O
33 ¹⁵ (+5)	[V ₂ O ₃ (phen) ₃ (Hcit) ₂ (phen) ₃ O ₃ V ₂]·12H ₂ O
34 ¹⁵ (+5)	[V ₂ O ₃ (phen) ₃ (<i>R,S</i> -H ₂ homocit)]Cl·6H ₂ O
35 ¹⁶ (+5)	K ₂ [V ₂ O ₄ (<i>R,S</i> -H ₂ homocit) ₂]·6H ₂ O
36 ¹⁶ (+3)	[Δ-V ^{III} ₄ V ^{IV} ₄ O ₅ (<i>R</i> -mal) ₆ (Hdatrz) ₆]·44.5H ₂ O
37 ¹⁶ (+3)	[Λ-V ^{III} ₄ V ^{IV} ₄ O ₅ (<i>S</i> -mal) ₆ (Hdatrz) ₆]·38.5H ₂ O
38 (+3)	K ₇ [V ^{III} ₅ V ^{IV} ₃ O ₅ (<i>R,S</i> -mal) ₆ (trz) ₆]·17H ₂ O

FeV-co in nitrogenases

39 ¹⁷⁽⁺³⁾	VFe ₇ S ₈ C(CO ₃)[<i>R</i> -(H)homocit] [PDB <i>5N6Y</i>]
40 ¹⁸⁽⁺³⁾	VFe ₇ S ₇ C(CO ₃)(OH)[<i>R</i> -(H)homocit] [PDB <i>6FEA</i>]
41 ¹⁹⁽⁺³⁾	VFe ₇ S ₈ C(CO ₃)[<i>R</i> -(H)homocit] [PDB <i>7ADR</i>]
42 ¹⁹⁽⁺³⁾	VFe ₇ S ₇ C(CO ₃)[<i>R</i> -(H)homocit] [PDB <i>7ADY</i>]
43 (+3)	VFe ₇ S ₇ C(CO ₃)(μCO)(tCO)[<i>R</i> -(H)homocit] [PDB <i>7AIZ</i>]

Abbreviation: bpz*eaT = 2,4-bis(3,5-dimethyl-1H-pyrazol-1-yl)-6-diethylamino-1,3,5-triazine; av = average

Table S10b. Comparisons of selected bond distances (Å) for oxidovanadium tartrates **1** – **18**, other oxidovanadium hydroxycarboxylates **19** – **38** and reported FeV-cos **39** – **43**.

Complexes (V ⁿ⁺)	V–O	V–O	V–O	V–N _{im}	C–O	C–O
	<i>α</i> -alkoxy	<i>α</i> -hydroxy	<i>α</i> -carboxy		<i>α</i> -alkoxy	<i>α</i> -hydroxy
1 (+4)	1.975(3) _{av}	2.237(3) _{av}	2.009(4) _{av}	2.128(4) _{av}	1.413(6) _{av}	1.418(6) _{av}
2 (+4)	1.976(2) _{av}		2.136(2) _{av}	2.117(3) _{av}	1.400(3) _{av}	
3 (+4)	1.980(2) _{av}	2.230(2) _{av}	2.013(2) _{av}	2.124(2) _{av}	1.411(3) _{av}	1.418(3) _{av}
4 (+4)	1.972(4) _{av}		2.137(4) _{av}	2.120(5) _{av}	1.406(6) _{av}	
5 ¹ (+4)	1.860(2) _{av}		2.020(2) _{av}		1.435(3) _{av}	
6 ² (+4)	1.910(6) _{av}		1.999(6) _{av}		1.409(9) _{av}	
7 ³ (+4)	1.917(2) _{av}		1.996(2) _{av}		1.401(4) _{av}	
8 ³ (+4)	1.914(2) _{av}		1.999(2) _{av}		1.412(4) _{av}	
9 ⁴ (+4)	1.912(1) _{av}		1.994(1) _{av}		1.408(4) _{av}	
10 ⁵ (+4)	1.934(3) _{av}		2.024(3) _{av}		1.392(4) _{av}	
11 ⁶ (+4)	1.961(2) _{av}	2.122(2) _{av}	1.999(2) _{av}		1.410(4) _{av}	1.428(4) _{av}
12 ⁶ (+4)	1.956(2) _{av}	2.238(2) _{av}	1.999(2) _{av}		1.410(3) _{av}	1.425(4) _{av}
13 ⁶ (+4)	1.970(4) _{av}	2.326(4)	1.990(4) _{av}		1.424(7) _{av}	1.441(7)
14 ⁶ (+4)	1.944(3) _{av}	2.306(3) _{av}	1.999(3) _{av}		1.416(5) _{av}	1.428(5) _{av}
15 ⁷ (+4)	1.806(3) _{av}		1.949(3) _{av}		1.396(5) _{av}	
16 ⁸ (+5)		2.272(2)	1.970(2)		1.426(3)	
17 ⁸ (+5)	1.825(2) _{av}		1.952(2) _{av}		1.414(2) _{av}	
18 ⁸ (+5)	1.820(1) _{av}		1.950(1) _{av}		1.409(2) _{av}	
19 ⁹ (+4)		2.231(2)	1.997(2)			1.422(4)
20 ⁹ (+4)	1.931(2)		2.018(2)		1.412(3)	
21 ⁹ (+4)	1.927(2)	2.244(2)	2.027(2) _{av}		1.410(4)	1.413(3)
22 ¹⁰ (+4)	1.976(5) _{av}		1.981(6)		1.424(5) _{av}	
23 ¹⁰ (+4)	2.108(2) _{av}		2.039(2)		1.423(2) _{av}	
24 ¹⁰ (+4)	2.077(2) _{av}		2.049(2) _{av}		1.429(2) _{av}	
25 ¹¹ (+4)		2.197(5)	1.993(4)			1.440(8)
26 ¹¹ (+4)		2.209(4)	1.983(3)			1.451(6)
27 ¹¹ (+4)		2.109(6) _{av}	2.026(6) _{av}			1.433(1) _{av}

28 ¹²⁽⁺⁴⁾		2.209(3)	1.994(3)		1.436(6)
29 ¹³⁽⁺⁵⁾	2.000(3)		1.957(3)	1.424(5)	
30 ¹⁴⁽⁺⁵⁾	2.026(1) _{av}		1.977(2)	1.422(2) _{av}	
31 ¹⁴⁽⁺⁵⁾	1.981(2) _{av}		2.004(2)	1.423(2) _{av}	
32 ¹⁵⁽⁺⁵⁾	1.851(4)		2.082(4)	1.432(8)	
33 ¹⁵⁽⁺⁵⁾	1.858(1)		2.072(1)	1.410(2)	
34 ¹⁵⁽⁺⁵⁾	1.858(4)		2.085(4)	1.410(7)	
35 ¹⁶⁽⁺⁵⁾	1.980(8) _{av}		1.959(8) _{av}	1.463(8) _{av}	
36 ¹⁶⁽⁺³⁾	1.992(4)			1.419(7)	
37 ¹⁶⁽⁺³⁾	1.994(4)			1.404(8)	
38 ¹⁶⁽⁺³⁾	2.005(2) _{av}			1.419(4)	
39 ¹⁷⁽⁺³⁾		2.170	2.112	2.304	1.436
40 ¹⁸⁽⁺³⁾		2.160	2.104	2.251	1.449
41 ¹⁹⁽⁺³⁾		2.146	2.112	2.267	1.456
42 ¹⁹⁽⁺³⁾		2.143	2.115	2.263	1.438
43 ²⁰⁽⁺³⁾		2.163	2.117	2.270	1.438

Table S11. Comparisons of Mo–O distances (Å) in typical molybdenum citrates with bridging sulfur/oxygen atom.

Complexes	Mo–O _α -alkoxy	Mo–O _α - carboxy
Mo–μ ₂ –S		
K _{2.5} Na ₂ NH ₄ [Mo ^V ₂ O ₂ S ₂ (cit) ₂]·5H ₂ O ²¹	2.021(8) _{av}	2.130(1) _{av}
K ₄ (NH ₄) ₂ [Mo ^V ₂ O ₂ S ₂ (cit) ₂]·10H ₂ O ²²	1.975(8)	2.199(9)
K ₅ (NH ₄)[Mo ^V ₂ O ₂ S ₂ (cit) ₂]·CH ₃ OH·5H ₂ O ²³	1.994(5) _{av}	2.192(5) _{av}
Mo–μ ₂ –O		
(NH ₄) ₆ [Mo ^V ₂ O ₄ (cit) ₂]·3H ₂ O ²⁴	2.016(4)	2.152(3)

Table S12. Bond valence calculations for complexes $(\text{H}_2\text{im})_2[\Delta, \Lambda\text{-V}^{\text{IV}}_2\text{O}_2(\text{R}, \text{R-H}_2\text{tart})(\text{R}, \text{R-tart})(\text{Him})_2] \cdot \text{Him}$ (**1**), $[\Lambda, \Lambda\text{-V}^{\text{IV}}_2\text{O}_2(\text{R}, \text{R-tart})(\text{Him})_6] \cdot 4\text{H}_2\text{O}$ (**2**), $(\text{H}_2\text{im})_2[\Lambda, \Delta\text{-V}^{\text{IV}}_2\text{O}_2(\text{S}, \text{S-H}_2\text{tart})(\text{S}, \text{S-tart})(\text{Him})_2] \cdot \text{Him}$ (**3**) and $[\Delta, \Delta\text{-V}^{\text{IV}}_2\text{O}_2(\text{S}, \text{S-tart})(\text{Him})_6] \cdot 4\text{H}_2\text{O}$ (**4**), respectively.

Complexes	Atoms	N	$\sum S_{ij}$	Δ
$(\text{H}_2\text{im})_2[\Delta, \Lambda\text{-V}^{\text{IV}}_2\text{O}_2(\text{R}, \text{R-H}_2\text{tart})(\text{R}, \text{R-tart})(\text{Him})_2] \cdot \text{Him}$ (1)	V(1)	4+	4.138	0.138
	V(2)	4+	4.148	0.148
$[\Lambda, \Lambda\text{-V}^{\text{IV}}_2\text{O}_2(\text{R}, \text{R-tart})(\text{Him})_6] \cdot 4\text{H}_2\text{O}$ (2)	V(1)	4+	4.099	0.099
	V(2)	4+	4.162	0.162
$(\text{H}_2\text{im})_2[\Lambda, \Delta\text{-V}^{\text{IV}}_2\text{O}_2(\text{S}, \text{S-H}_2\text{tart})(\text{S}, \text{S-tart})(\text{Him})_2] \cdot \text{Him}$ (3)	V(1)	4+	4.116	0.116
	V(2)	4+	4.117	0.117
$[\Delta, \Delta\text{-V}^{\text{IV}}_2\text{O}_2(\text{S}, \text{S-tart})(\text{Him})_6] \cdot 4\text{H}_2\text{O}$ (4)	V(1)	4+	4.185	0.185
	V(2)	4+	4.130	0.130

References

1. J. G. Forrest and C. K. Prout, *J. Chem. Soc. A*, 1967, 1312–1317.
2. R. E. Tapscott, R. L. Belford and I. C. Paul, *Inorg. Chem.*, 1968, **7**, 356–364.
3. J. T. Wroblewski and M. R. Thompson, *Inorg. Chim. Acta*, 1988, **150**, 269–277.
4. J. Garcia Jaca, T. Rojo, J. L. Pizarro, A. Goñi and M. I. Arriortua, *J. Coord. Chem.*, 1993, **30**, 327–336.
5. R. B. Ortega, C. F. Campana and R. E. Tapscott, *Acta. Crystallogr. B*, 1980, **B36**, 1786–1788.
6. A. J. Cortese, B. Wilkins, M. D. Smith, J. Yeon, G. Morrison, T. T. Tran, P. S. Halasyamani and H. C. zur Loye, *Inorg. Chem.*, 2015, **54**, 4011–4020.
7. X. T. Ma, N. Xing, Z. D. Yan, X. X. Zhang, Q. Wu and Y. H. Xing, *New J. Chem.*, 2015, **39**, 1067–1074.
8. J. Galikova, P. Schwendt, J. Tatiarsky, A. S. Tracey and Z. Zak, *Inorg. Chem.*, 2009, **48**, 8423–8430.
9. W. T. Jin, H. Wang, S. Y. Wang, C. H. Dapper, X. Li, W. E. Newton, Z. H. Zhou and S. P. Cramer, *Inorg. Chem.*, 2019, **58**, 2523–2532.
10. M. Tsaramyrsi, M. Kaliva, A. Salifoglou, C. P. Raptopoulou, A. Terzis, V. Tangoulis and J. Giapintzakis, *Inorg. Chem.*, 2001, **40**, 5772–5779.
11. C. Y. Chen, M. L. Chen, H. B. Chen, H. Wang, S. P. Cramer and Z. H. Zhou, *J. Inorg. Biochem.*, 2014, **141**, 114–120.
12. V. Jodaian, M. Mirzaei, M. Arca, M. Carla Aragoni, V. Lippolis, E. Tavakoli and N. S. Langeroodi, *Inorg. Chim. Acta*, 2013, **400**, 107–114.
13. M. Tsaramyrsi, D. Kavousanaki, C. P. Raptopoulou, A. Terzis and A. Salifoglou, *Inorg. Chim. Acta*, 2001, **320**, 47–59.
14. M. Kaliva, C. P. Raptopoulou, A. Terzis and A. Salifoglou, *J. Inorg. Biochem.*, 2003, **93**, 161–173.
15. C. Y. Chen, Z. H. Zhou, H. B. Chen, P. Q. Huang, K. R. Tsai and Y. L. Chow, *Inorg. Chem.*, 2008, **47**, 8714–8720.
16. D. W. Wright, R. T. Chang, S. K. Mandal, W. H. Armstrong and W. H. Orme-Johnson, *J. Biol. Inorg. Chem.*, 1996, **1**, 143–151.
17. D. Sippel and O. Einsle, *Nat. Chem. Bio.*, 2017, **13**, 956–960.
18. D. Sippel, M. Rohde, J. Netzer, C. Trncik, J. Gies, K. Grunau, I. Djurdjevic, L. Decamps, S. L. A. Andrade and O. Einsle, *Science*, 2018, **359**, 1484–1489.
19. M. Rohde, K. Grunau and O. Einsle, *Angew. Chem. In. Ed.*, 2020, **59**, 1–6.
20. M. Rohde, K. Laun, I. Zebger, S. T. Stripp and O. Einsle, *Sci. Adv.*, 2021, **7**, eabg4474.
21. Y. H. Xing, J. Q. Xu, H. R. Sun, D. M. Li, Y. Xing, Y. H. Lin and H. Q. Jia, *Eur. J. Solid State Inorg. Chem.*, 1998, **35**, 745–756.
22. D. M. Li, Y. H. Xing, Z. C. Li, J. Q. Xu, W. B. Song, T. G. Wang, G. D. Yang, N. H. Hu, H. Q. Jia and H. M. Zhang, *J. Inorg. Biochem.*, 2005, **99**, 1602–1610.
23. J. Q. Xu, X. H. Zhou, L. M. Zhou, T. G. Wang, X. Y. Huang and B. A. Averill, *Inorg. Chim. Acta*, 1999, **285**, 152–154.
24. Z. H. Zhou, Y. F. Deng, Z. X. Cao, R. H. Zhang and Y. L. Chow, *Inorg. Chem.*,

2005, **44**, 6912–6914.